Modern Physics Letters B, Vol. 24, No. 15 (2010) 1675–1689

DOI: 10.1142/S0217984910024080

World Scientific
www.worldscientific.com

QUANTUM DOT GEOMETRY AS A DESIGNING TOOL FOR DOT-IN-A-WELL STRUCTURES

NASRINDOKHT BATENIPOUR

Department of Electrical Engineering, Sciences and Research Branch, Islamic Azad University, Tehran, 1477893855, Iran
batenipour_nd@srbiau.ac.ir

KAMYAR SAGHAFI*

Department of Electrical Engineering, Shahed University, P. O. Box 18155-159, Tehran, Iran
saghafi@shahed.ac.ir

M. K. MORAVVEJ-FARSHI

Advanced Device Simulation Lab (ADSL), Department of Electrical and Computer Engineering, Tarbiat Modares University (TMU), P. O. Box 14115-143, Tehran 1411713116, Iran
farshi_k@modares.ac.ir

Received 11 August 2009

In this paper, we report results of our investigation on the effect of quantum dot (QD) geometry on desirable properties of a dot-in-a-well (DWELL) structure. Our simulation results reveal that QD geometry plays a key role in tuning the electronic properties of DWELL structure and can be employed as a designing tool. The structure under investigation consists of an InAs QD confined in an InGaAs well of size ∼12.3 nm which in turn is sandwiched in a GaAs bulk. Using the path integral Monte Carlo (PIMC) method, we calculate the electronic properties of DWELL structure for QDs of spherical, ellipsoidal, and conical shapes. We demonstrate the dependence of the electron energy on QD geometry. We show that although the stronger confinement within the conical quantum dot (CQD) forces its maximum capacity ($N_{\max}$) to be smaller than those of the spherical quantum dot (SQD) and ellipsoidal quantum dot (EQD), the overall maximum capacity of a DWELL with conical dot (CDWELL) is larger than those of the DWELLs with spherical and ellipsoidal dots (SDWELL and EDWELL). Moreover, we show that the electron distribution within the structure is a strong function of the QD geometry inside the well.

Keywords: Dot-in-a-well; path integral Monte Carlo; quantum dot; quantum well.

*Corresponding author.

1. Introduction

Quantum dots (QDs) are three-dimensional (3D) electronic systems confined in strong attractive potentials similar to the nucleus of atoms.[1] Such confining potentials are responsible for atomic-like electronic properties of QDs. One may tune properties of a QD, by tailoring its confining potential. In this regard, a QD can be viewed as an artificial atom.

Tunable electronic properties of QD structures as well as their wide variety of applications in electronics and optoelectronics have made them of great interest to both theoretical and experimental research groups. For example, Reimann and Manninen[2] have already presented an extensive review on electronic structure of QDs.

QDs have discrete energy levels with large density of states desirable for high performance optoelectronic devices. Krishna[3] and Amtout *et al.*[4] have already reported theoretical and experimental results on photodetectors made of InAs QDs embedded in an InGaAs quantum well (QW). These detectors represent a hybrid between a QD detector and a QW detector. Confining potentials in such structures which are responsible for the device behavior are influenced by both QW and QD material compositions and geometries. Although, the effects of the QD material composition and geometry on its electronic properties have already been studied extensively,[5–14] similar reports on dot-in-a-well (DWELL) are limited to those of Refs. 3 and 4, in which the QD shape effect has not been investigated. In the case of DWELL, electronic properties of QD are modified in the influence of the well confinement. Moreover, QD shape not only affects electronic structure of QD but also alters effective well confinement and consequently electronic properties of the whole DWELL structure. So, there is a mutual relation between QD and QW. In this paper, we have considered the QD geometry as a tool for designing DWELL electronic structures. Using the path integral Monte Carlo (PIMC) method,[15–17] we have studied the electronic properties of InAs/InGaAs/GaAs spherical dot-in-a-well (SDWELL), ellipsoidal dot-in-a-well (EDWELL), and conical dot-in-a-well (CDWELL) structures. Spherical, ellipsoidal, and conical QDs in InAs/GaAs material composition have been reported earlier,[18–24] hence we select these QD shapes for our investigation. To compare the electronic properties of these structures, the dots volume and the wells width for all three DWELLs are taken to be the same.

The rest of this paper is organized as follows. In Sec. 2, we present a Hamiltonian model for SDWELL, EDWELL, and CDWELL, each containing N electrons interacting with each other. Section 3 describes DWELL structure geometry and simulation method. In Sec. 4, we present the results and discussions. Finally, we close this paper by conclusion, in Sec. 5.

2. Modeling DWELL Structures

A DWELL configuration is a many-body system containing N electrons, those Hamiltonian is modeled by summation over Hamiltonians of N electrons in the

confining potential plus the effects of the columbic interactions among the electrons,[17]

$$\hat{H} = \sum_{i=1}^{N} \left[-\frac{\hbar^2}{2m^*} \nabla_i^2 + V(r_i) \right] + \sum_{j<i}^{N} \frac{e^2}{4\pi\varepsilon_r \varepsilon_0 \left| r_i - r_j \right|} \,. \tag{1}$$

where m^* is the electron effective mass, $r_i = (x_i, y_i, z_i)$ is the position of ith electron, $\hbar = h/2\pi$ is the reduced Planck constant, e is the electronic charge, ε_r is the relative material dielectric constant, ε_0 is the free space dielectric constant, $|r_i - r_j|$ is the spatial distance between ith and jth electrons and $V(r_i) = V_D(r_i) + V_W(r_i)$ is the total confining potential; where $V_D(r_i)$, and $V_W(r_i)$ are dot and well-confining potentials, respectively, seen by the ith electron. The first summation in Eq. (1) represents the kinetic and potential energies of the system, while the second summation corresponds to the electron–electron (e–e) interactions. The effect of such a repulsive potential, contrary to that of the total confining potential, is to spread the electrons through out the dot.

In this simulation, we have considered a QW with a z-directed confining potential

$$V_W(r_i) = a_w[1 - \exp(-b_w z_i^{2c_w})] \,, \tag{2}$$

where a_w is the well height defined by the conduction band discontinuity (ΔE_C) existing between the well and the bulk materials, and b_w and c_w are positive constants, representing the well parameters that tune the well width and slope, respectively. In the present work, we have chosen $c_w = 4$ which results in a nearly square-shaped potential.

Confining potentials of various profiles have already been used for describing quantum dots of various shapes.[5–14,25,26] In many cases, however, the maximum potential at the dot boundary is considered to be equal to the band discontinuity, ΔE_C, between the dot and the surrounding materials.[25,26] In our model, an ellipsoidal QD (EQD) is defined by

$$V_{\mathrm{EQD}}(r_i) = \begin{cases} \dfrac{(\Gamma\omega_0)^2 (a_d x_i^2 + b_d y_i^2 + c_d z_i^2)}{2} & \text{inside EQD} \\ \Delta E_C & \text{outside EQD} \end{cases} , \tag{3}$$

where a_d, b_d, and c_d are positive constants, ω_0 is the oscillation frequency and Γ is a correction factor for tuning QD size. To obtain the confining potential for a spherical QD (SQD), however, one should set $a_d = b_d = c_d$ in Eq. (3), which results in

$$V_{\mathrm{SQD}}(r_i) = \begin{cases} \dfrac{(\Gamma\omega_0)^2 a_d\, r_i^2}{2} & \text{inside SQD} \\ \Delta E_C & \text{outside SQD} \end{cases} , \tag{4}$$

where $r_i^2 = (x_i^2 + y_i^2 + z_i^2)$.

The confining potential for a conical QD (CQD) is

$$V_{\mathrm{CQD}}(r_i) = \begin{cases} \dfrac{(\Gamma\omega_0)^2[a_d x_i^2 + b_d y_i^2 - c_d^+(z_i - z_0^+)^2 + c_d^+ z_0^{+2}]}{2} & \text{inside CQD for } 0 \le z_i \le z_0^+ \\ \dfrac{(\Gamma\omega_0)^2[a_d x_i^2 + b_d y_i^2 - c_d^-(z_i - z_0^-)^2 + c_d^- z_0^{-2}]}{2} & \text{inside CQD for } z_0^- \le z_i < 0 \\ \Delta E_C & \text{outside CQD} \end{cases} \tag{5}$$

where a_d, b_d, c_d^+, c_d^-, and z_0^+ are positive constants while z_0^- is a negative constant. Inside CQD, z_i varies between z_0^- and z_0^+. Actually, this CQD consists of a cone and an inverted cone, whose axes are in z-direction while their common base is in the x–y plane. To have a circular base, one should set $a_d = b_d$. The cone vertexes are defined by $x_i = y_i = 0$ and $z_i = z_0^+$, z_0^- with maximum potential. Satisfying continuity condition at cone vertexes; i.e. $V_{\mathrm{CQD}}(0, 0, z_0^-) = V_{\mathrm{CQD}}(0, 0, z_0^+) = \Delta E_C$, leads to

$$\frac{c_d^+}{c_d^-} = \left(\frac{z_0^-}{z_0^+}\right)^2. \tag{6}$$

3. DWELL Structure Geometry and Simulation Method

Figure 1 illustrates 3D schematics of the example SDWELL, EDWELL, and CDWELL structures as well as their respective confining potentials.

All three DWELL structures are made of same materials, with an InAs QD inside a GaAs/$In_{0.15}Ga_{0.85}As$/GaAs square QW of 12.3 nm wide, embedded in a cubic GaAs of volume (18.6 nm).[3] Using material parameters given in Table 1, extracted from Refs. 27 and 28, and assuming that $\Delta E_C = 0.6\Delta E_g$ for both InAs/InGaAs and GaAs/InGaAs, the dot and well maximum confining potentials, respectively, become $\Delta E_{CD} = 547.2$ meV and $\Delta E_{CW} = 97.2$ meV.

For the sake of simplicity we have normalized energies and lengths by $\hbar\omega_0 = 10$ meV and $\ell_0 = (\hbar/m_D^*\omega_0)^{1/2} = 18.6$ nm, respectively. Performing such normalization, the Hamiltonian operator of Eq. (1) reduces to

$$\hat{H} = \sum_{i=1}^{N}\left[-\frac{1}{2}\nabla_i^2 + \frac{m^*}{m_D^*}V(r_i)\right] + \sum_{j<i}^{N}\frac{\Lambda}{|r_i - r_j|}, \tag{7}$$

where m_D^* is the electron effective mass in the dot, $\Lambda = \ell_0/a_B^*$ is a dimensionless parameter known as the coupling constant, that describes e–e interaction, and $a_B^* = (e^2 m^*)/(4\pi\varepsilon_r\varepsilon_0\hbar^2)$ is the material effective Bohr radius.[1] Constants a_B^* and Λ are both material dependent, whose values for InAs, GaAs, and $In_{0.15}Ga_{0.85}As$ are given in Table 1.

We calculate desirable properties of DWELL structure using $3N$ dimensional Hamiltonian model of Eq. (7). Path integral Monte Carlo (PIMC) method is a

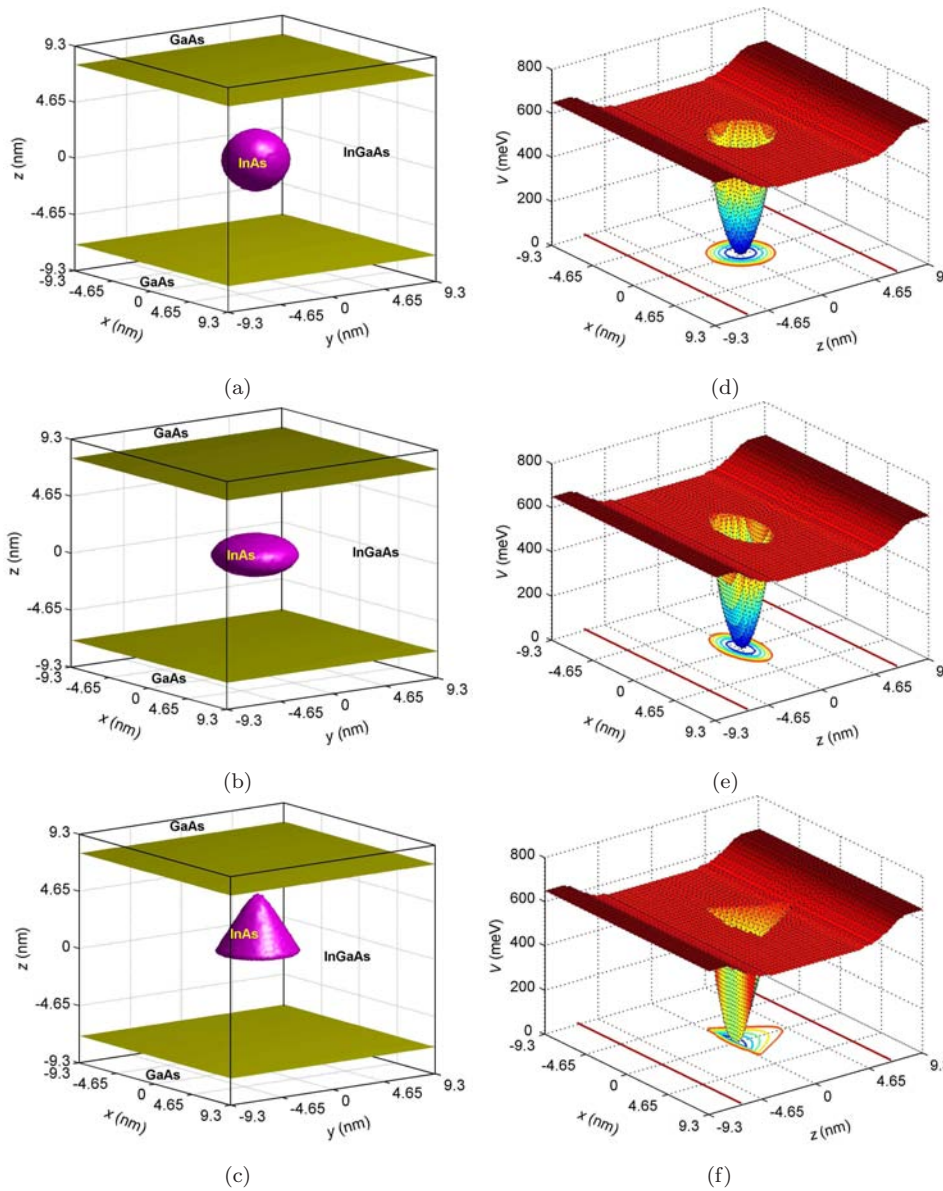

Fig. 1. (Color online) Schematics of structures for (a) SDWELL, (b) EDWELL, (c) CDWELL and their corresponding confining potentials illustrated in (d), (e), and (f), respectively. The confining potentials are shown for x–z plane, at $y = 0$, with their minima are all at origin, i.e. $x = y = z = 0$.

powerful Quantum Monte Carlo (QMC) technique for simulation of many-body interacting systems. It is based on density matrix calculation and isomorphism theorem that maps a quantum particle to a ring of classical particles. It describes low temperature (quantum particle) density matrix in terms of a product of high

Table 1. Material parameters for InAs, GaAs, and $In_{0.15}Ga_{0.85}As$ extracted from Refs. 27 and 28.

Parameter	Symbol	Material			Unit
		InAs	GaAs	$In_{0.15}Ga_{0.85}As$	
Band gap (at $T = 300$ K)	E_g	0.36	1.425	1.264	eV
Band gap (at $T = 77$ K)		0.438	1.512	1.350	eV
	$\Delta E_g/\Delta T$	−0.35	−0.39	−0.384	meV
Electron effective mass	m^*	0.022	0.066	0.060	—
Relative dielectric constant	ε_r	15.1	13.2	13.5	—
Effective Bohr radius	a_B^*	36.3	10.5	11.9	nm
Coupling constant[a]	Λ	0.51	1.76	1.56	—

[a]Calculated for each material.

temperature (classical particle) density matrices.[16,17] We apply this simulation method for its capability to consider e–e interactions directly and to solve many dimensional problem with less approximations.

We employ the simple case of distinguishable particles to avoid computational complexity; however, we calculate e–e interactions for different materials accurately. Common PIMC algorithms utilize an average value for effective mass and dielectric constant in heterostructures of different materials. We improve the algorithm to include material dependent parameters instead of using constant approximate average values. In our algorithm, material parameters of Eq. (7) change according to the place of particles (electrons). Therefore, during the simulation, while an electron cross the boundary between different materials, its effective mass and coupling constant alter according to Table 1. Moreover, to have fixed number of electrons, when electron cross simulation box boundary from one side, it is replaced by another electron from the other side. Using Li–Broughton action and virial energy estimator,[15] our algorithm converges with timestep 0.03 $(\text{meV})^{-1}$ at $T = 77$ K.

4. Results and Discussions

Using the PIMC method and Hamiltonian model of Eq. (7), we have simulated three DWELL structures of Fig. 1 at $T = 77$ K. In this simulation, we have used a normalization volume of $V_0 = (4\pi R_0^3/3)$ that corresponds to an SQD of radius $R_0 = 2.4$ nm, as a reference QD size for comparing results obtained from QDs of various geometries.

First, we examine the strength of confining potentials experienced by electrons within three different DWELLs of Fig. 1. Figure 2 illustrates the total energy, E_T, potential energy, PE, and kinetic energy, KE, (all per electron) versus the number of electrons, N, for the three DWELL structures, having QDs of the same size V_0.

This figure demonstrates that E_T and PE, for all three DWELL structures, are increasing functions of N. This is due to the fact that by increasing the number of electrons, the e–e repulsive interaction is enhanced and forces the electrons to

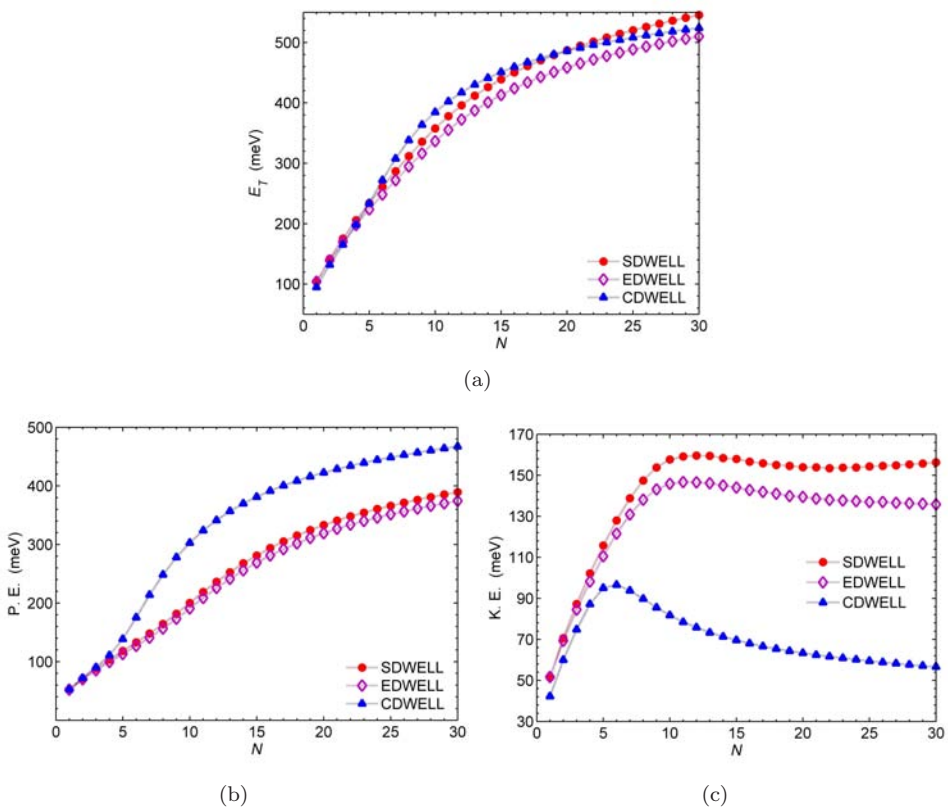

Fig. 2. Variations of (a) E_T, (b) PE, and (c) KE, for three DWELL structures all with QDs of the same size V_0, in terms of number of electrons, N.

spread out within the structure residing in higher energy levels. Kinetic energy also increases by N, first, whilst electrons are inside the dot. It, however, starts to decrease beyond a maximum value for N (i.e. $N > N_{\max}$). In fact, $N_{\max}$ determines the dot capacity, beyond which at least one electron moves out of the dot into the surrounding well, with smaller confining potential.

Furthermore, we observe that for $N > 5$, PE for the CDWELL is at least 20% larger than that for both SDWELL and EDWELL. In fact, this is due to stronger electron confinement in CQD that raises the electron energy. Energy increment is in the form of potential and strong confinement in CQD resisting against electron movement; hence, resulting in lowest KE for CDWELL among the three structures under consideration. We can also see that PE for SDWELL is only slightly more than that for the example EDWELL — at most 5%. It is due to 3D symmetry of confining potential in SQD that confines electrons in all three directions in the same manner; while the 2D symmetry of confining potential in the example EQD confines electrons in the x–y plane less than that it does in the z direction. The overall confinement by the example EQD is, however, less than that of SQD. Hence

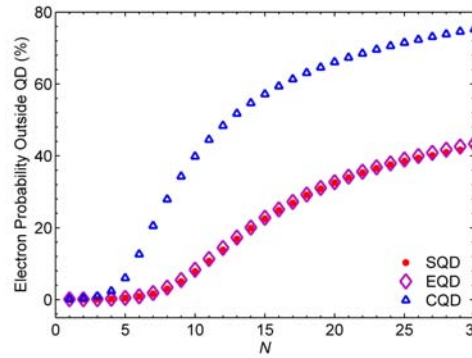

Fig. 3. Probabilities of electron moving out from SQD, EQD, and CQD into the surrounding QW, as function of N. All QDs have the same volume V_0.

SDWELL has stronger overall confinement and consequently higher energy in both potential and kinetic forms, in comparison to the example EDWELL. Although strong confinement tends to limit electron movement, in general, inherent symmetry of SQD eases the electron movement in SDWELL, resulting in a higher KE than EDWELL.

To find the maximum electron capacity ($N_{\max}$) for each of the three aforementioned QDs, then, we have calculated the probability of electrons being forced out of each QD, into the surrounding QW as a function of N. Figure 3 compares such probabilities for three QDs of the same size V_0. To our expectation, Fig. 3 shows that as the number of electrons in each QD increases, the probability of an electron moving from the dot into the surrounding QW with a weaker confining potential increases. Such an increase, however, varies with the QD shape. As seen in this figure, the stronger the confining potential the higher is the probability of electron moving out of the dot. Hence, probability of electrons moving outside CQD is larger than the probabilities for EQD and SQD of the same size.

Table 2 shows $N_{\max}$ and its corresponding total energy (E_T) and potential energy for DWELL structure with SQD, EQD, and CQD of volume V_0, $2V_0$, and $3V_0$. For all QD shapes by enlarging the dot, $N_{\max}$ increases while corresponding potential energy percentage decreases. Therefore, in large QDs electrons need more kinetic energy for coming out of quantum dot. As expected, CQD has smaller $N_{\max}$ and confines fewer electrons. Electron confinement in CQD is strong even in large sizes. This leads to high energy electrons and therefore small $N_{\max}$.

Next, we have examined the dependence of the total energy (E_T) per electron for each of the three aforementioned DWELLs on the corresponding QD size, normalized to V_0, with N as varying parameter. In each case, E_Ts are compared with those of similar QDs embedded in $In_{0.15}Ga_{0.85}As$ bulks, in absence of QWs. Number of electrons are chosen such that the number of electrons outside the QD of size V_0 is 0, 1, 2, or 3. The corresponding Ns for such a CQD are 3, 7, 8, and 9, respectively. These numbers, for an equal size EQD/SQD are 4, 11, 13, and 15, respectively.

Table 2. Maximum number of QD confined electrons ($N_{\max}$) and their related energies for SDWELL, EDWELL, and CDWELL of various QD sizes.

QD Type	Volume	$N_{\max}$	E_T (meV)	PE (meV)	PE/E_T(%)
SQD	V_0	10	357.8	200.1	55.93
SQD	$2V_0$	15	397.9	212.3	53.36
SQD	$3V_0$	20	436.0	229.2	52.56
EQD	V_0	10	336.7	190.8	56.68
EQD	$2V_0$	15	366.7	198.6	54.15
EQD	$3V_0$	20	394.5	210.3	53.29
CQD	V_0	6	272.1	175.5	64.50
CQD	$2V_0$	7	269.2	164.5	61.11
CQD	$3V_0$	8	275.7	166.8	60.52

To our expectation, Fig. 4 demonstrates that by increasing QD size, in each case, confining effect becomes weaker and hence the total energy decreases. Furthermore, we can observe that the presence of QW increases the confinement and enhances the total energy as a consequence. Such an effect becomes negligible in extreme cases in which either number of electrons is small or the size of QD is large, enough to make the probability of electrons moving outside the QD negligible. On the other hand, when either the number of electrons are large or the size of QD is small enough to make the aforementioned probability countable, presence of QW enhances the confining and hence the total energy. Comparison of the three cases, shown in Fig. 4, reveals that while the presence of QW in a CDWELL with a QD of volume $V \leq 3V_0$ containing $N \geq 7$ electrons becomes effective, for other two structures this effect becomes pronounced for a QD of volume V_0 containing $N \geq 11$ electrons or volume $2V_0$ containing $N \geq 15$ electrons.

The total energy of a DWELL system containing N electrons, $U(N) = E_T \cdot N$, increases by adding an electron to it. The minimum energy for adding the Nth electron to the system, $\mu(N)$, is called electrochemical potential or electron energy level and defined as[11,29]

$$\mu(N) = U(N) - U(N-1)\,. \tag{8}$$

Figure 5 illustrates the electrochemical potential of CDWELL, EDWELL, and SDWELL structures. As shown in the figure, in general, $\mu(N)$ increases by N. Its value exceeds the confining potential ($\Delta E_{CD} = 547.2$ meV) when number of electrons exceeds $N = 8$ for CQD, $N = 10$ for SQD, and $N = 12$ for EQD. Energy levels below the confining potential (i.e. $\mu < \Delta E_{CD}$) correspond to the electrons inside QD, while higher energy levels correspond to the electrons outside the dot, within the surrounding well. As can be seen from this figure, energy levels inside CQD are higher than their corresponding levels inside SQD which in turn are higher than those of EQD. Outside the dot the situation alters, such that for

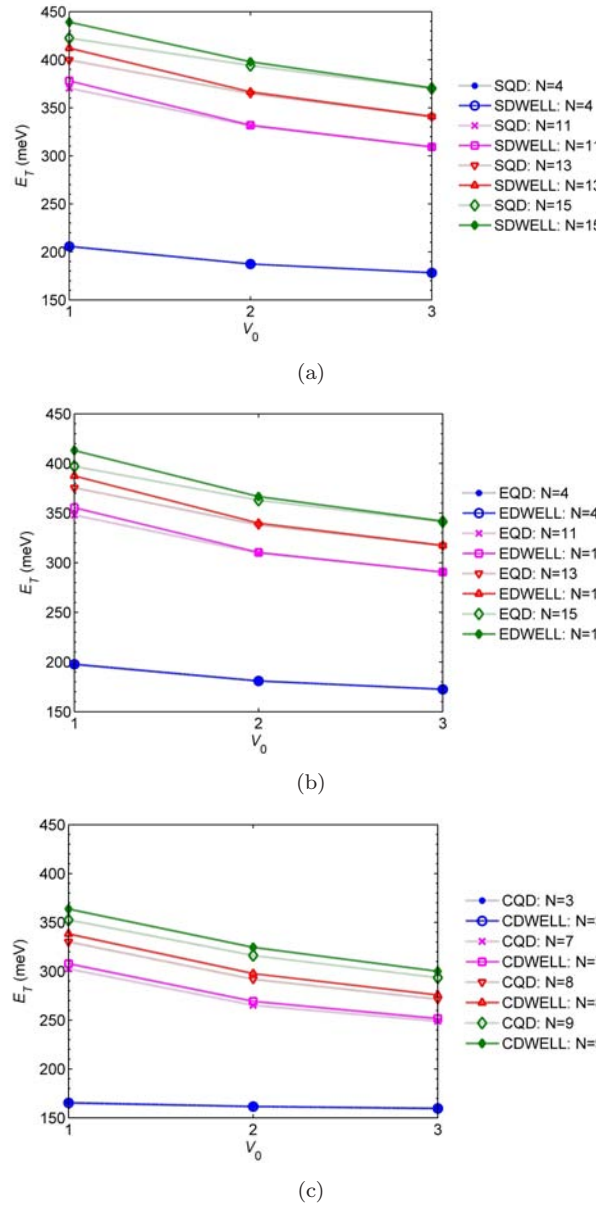

Fig. 4. Total energy per electron, E_T, for (a) SDWELL, (b) EDWELL, and (c) CDWELL, containing various numbers of electrons, as functions of dot volume normalized to V_0, compared with those of corresponding QDs in absence of QW.

large Ns confinement by SDWELL is the strongest and that of the CDWELL is the weakest. This will be enlightened more, when we present the results on addition energy.

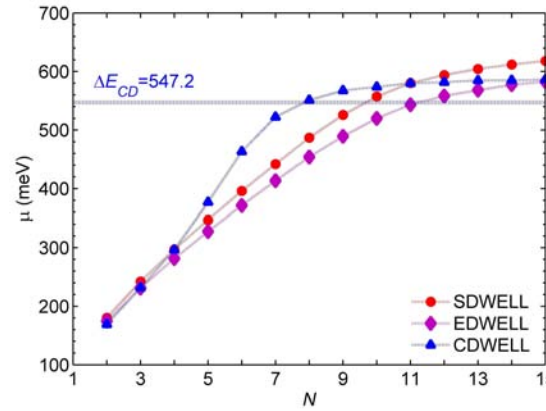

Fig. 5. Electrochemical potential for SDWELL, EDWELL, and CDWELL structures, with QDs of volume V_0.

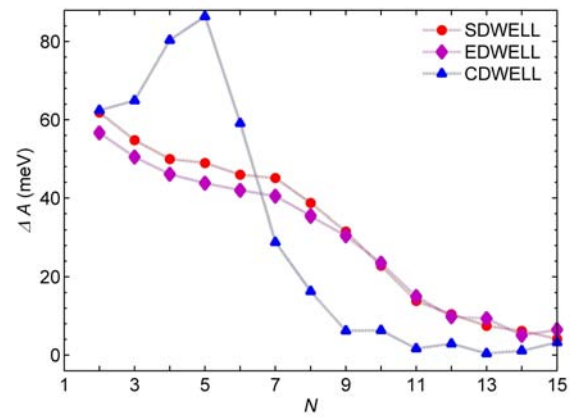

Fig. 6. Addition energy for SDWELL, EDWELL, and CDWELL structures, with QDs of volume V_0.

Addition or capacitive energy is another parameter for evaluating electronic properties of QD systems. It is equivalent to the energy gap between the lowest unoccupied and highest occupied states for an N-electron QD system and can be defined as[11,29]

$$\Delta A(N) = \mu(N+1) - \mu(N) = U(N+1) + U(N-1) - 2U(N)\,. \tag{9}$$

Figure 6 shows the addition energy for all three DWELL structures. Due to strong confinement of CQD for $N \leq N_{\max}$, separation between its energy levels are large, and hence the addition energy for $N \leq N_{\max}$ is significant in the CDWELL structure. Beyond $N_{\max}$, however, the addition energy drops, suddenly. This sudden drop, which can be observed for all three cases, is due to the fact that the

confinements resulted from the 1D QWs are weaker than those of the 3D QDs. Furthermore, one can observe that this drop in addition energy for CDWELL is sharper than those for SDWELL and EDWELL. This is because, the QW energy levels which accommodate the added electrons ($N - N_{\max}$) are determined by the well effective width, which in turn is affected by the geometry of QD. From Fig. 6, we can conclude that the well effective width in presence of CQD is larger than those in presence of SQD and EQD, and hence the separation between energy levels in the well surrounding CQD (the CDWELL addition energy for $N > N_{\max}$) is less than those corresponding to SDWELL and EDWELL. This behavior alters the probability of electrons remaining within the DWELL for $N > N_{\max}$, such that the maximum capacities for SDWELL and EDWELL are both about 13, while for CDWELL it is about 14. That is beyond these numbers, at least one electron moves out of the corresponding DWELL structure, into the GaAs.

Confining potential, in any system, affects the electron distribution within that structure. Such an effect is illustrated in Fig. 7 which presents the electron distributions within SDWELL, EDWELL, and CDWELL structures, for $N = 40$. The illustration presents 2D distributions with 3D insets. As it is evident, from these figures, electron distribution, in each case, obeys the confining potential profile and its symmetry. For SDWELL and EDWELL almost 50% of the electrons are distributed within the dot; while for CDWELL only 20% of the electrons are confined inside the dot. As can be seen further, from Fig. 7(b), electrons moving out of the EQD confining potential pile up on the top and bottom sides of the dot, in the z-direction, inside the surrounding QW. This also can be observed from the inset. Figure 7(c) demonstrate that most of the confined electrons distributed inside the CQD are concentrated around the cone base, while a small portion of them distributed within the upper part of the CQD. Meanwhile, almost all of the electrons that moved out of the CQD are distributed in the lower part of the QW, beneath the CQD. While in the other two structures, such electrons are distributed all around the dots.

5. Conclusion

We have reported PIMC simulation of SDWELL, EDWELL, and CDWELL structures. Such structures consist of InAs QDs with spherical, ellipsoidal, or conical geometry of the same volume $V_0 = 57.9$ nm^3, $2V_0$, or $3V_0$, each embedded in an $In_{0.15}Ga_{0.85}As$-QW of width ~ 12.3 nm which in turn is sandwiched in a cubic shape GaAs barriers of outer sides ~ 18.6 nm. In this study, we have demonstrated that the effect of QD geometry can be employed as a tool in tailoring confining potential and tuning electronic properties of the DWELL structures.

By varying the QD size, while keeping size of the other elements of DWELL structure fixed, we have studied the dependence of the electron energy on the QD size, and observed that the total energy per electron is a decreasing function of QD volume.

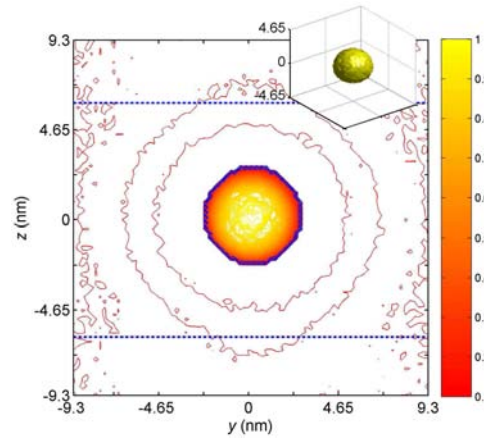

(a)

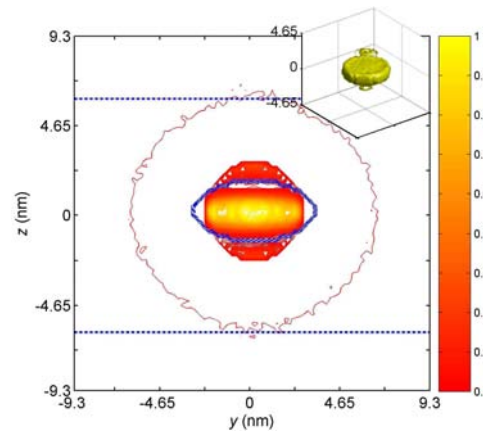

(b)

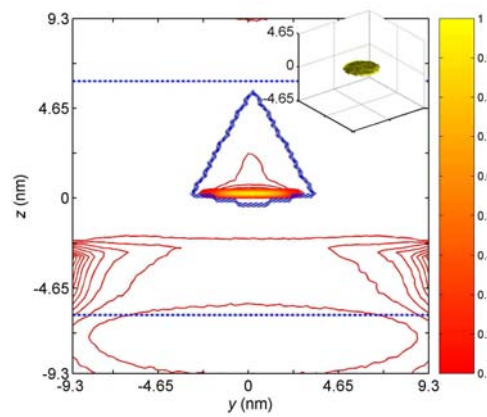

(c)

Fig. 7. (Color online) A 2D view of electron distribution throughout (a) SDWELL, (b) EDWELL, and (c) CDWELL structures, for $N = 40$. The inset, in each case shows the 3D distribution.

We have also calculated and compared the total, potential, and kinetic energies per electron, electrochemical potential, and addition energy for the three DWELL structures, with QDs of the same volume V_0. Electrochemical potential and addition energy of the sample DWELL structures demonstrate to be strongly dependent upon the QD geometry. Furthermore, we have concluded that the well effective width in CDWELL is larger than those of the SDWELL and EDWELL.

Finally, by simulating the effect of QD geometry on electron distribution throughout the DWELL structures containing 40 electrons, we have observed that electron distribution follows the dot potential profile. Within a 3D symmetric profile such as SQD, in a SDWELL, electron distribution follows the symmetry. Distribution within the well surrounding SQD, although less concentrated, almost follows the same symmetry. In the EDWELL, electron distribution inside the EQD with a 2D symmetry also follows its potential profile, whereas outside the dot electrons are concentrated on the dot surface with less curvature. The distribution inside the dot within CDWELL is shown to be concentrated near the CQD base, while outside the dot it is concentrated more around the bottom surface with less curvature. Such results reveal that the dot geometry can play a key role in tuning the electronic properties of DWELL structures.

References

1. B. Reusch, Ph.D. thesis, Heinrich-Heine University, Düsseldorf, Germany, 2003.
2. S. M. Reimann and M. Manninen, *Rev. Mod. Phys.* **74** (2002) 1283.
3. S. Krishna, *J. Phys. D: Appl. Phys.* **38** (2005) 2142.
4. A. Amtout, S. Raghavan, P. Rotella, G. von Winckel, A. Stintz and S. Krishna, *J. Appl. Phys.* **96** (2004) 3782.
5. C. Pryor, *Phys. Rev. B* **60** (1999) 2869.
6. L. W. Wang, J. Kim and A. Zunger, *Phys. Rev. B* **59** (1999) 5678.
7. D. G. Austing, S. Sasaki, S. Tarucha, S. M. Reimann, M. Koskinen and M. Manninen, *Phys. Rev. B* **60** (1999) 11514.
8. A. J. Williamson, L. W. Wang and A. Zunger, *Phys. Rev. B* **62** (2000) 12963.
9. R. Pino and V. M. Villalba, *J. Phys.: Condens. Matt.* **13** (2001) 11651.
10. E. Räsänen, H. Saarikoski, V. N. Stavrou, A. Harju, M. J. Puska and R. M. Nieminen, *Phys. Rev. B* **67** (2003) 235307.
11. G. Cantele, F. Trani, D. Ninno and G. Iadonisi, *J. Phys.: Condens. Matt.* **15** (2003) 5715.
12. M. Sahin and M. Tomak, *Phys. Rev. B* **72** (2005) 125323.
13. J. H. Marín, F. J. Betancur and I. D. Mikhailov, *J. Phys. Condens. Matt.* **18** (2006) 1005.
14. B. Pujari, K. Joshi, D. G. Kanhere and S. A. Blundell, *Phys. Rev. B* **76** (2007) 085340.
15. L. B. Barberà, Ph.D. thesis, Universitat Politcnica de Catalunya, Barcelona, Italy, 2002.
16. D. M. Ceperley, *Rev. Mod. Phys.* **67** (1995) 279.
17. J. Shumway and D. M. Ceperley, in *Handbook of Theoretical and Computational Nanotechnology*, Vol. 3, eds. M. Rieth *et al.* (American Scientific Publishers, Los Angeles, 2006), pp. 605–641.
18. F. Grosse and R. Zimmermann, *Phys. Rev. B* **75** (2007) 235320.

19. Z. H. Dai, L. D. Zhang, J. Z. Sun, Z. H. Li and S. Y. Huang, *Appl. Phys. Lett.* **80** (2002) 2577.
20. Y. H. Zhu, X. W. Zhang and J. B. Xia, *Phys. Rev. B* **73** (2006) 165326.
21. J. H. Blokland, M. Bozkurt, J. M. Ulloa, D. Reuter, A. D. Wieck, P. M. Koenraad, P. C. M. Christianen and J. C. Maan, *Appl. Phys. Lett.* **94** (2009) 023107.
22. H. Leon, J. L. Marin and R. Riera, *Physica E* **27** (2005) 385.
23. H. She and B. Wang, *Semicond. Sci. Technol.* **24** (2009) 025002.
24. D. M. T. Kuo and Y. C. Chang, *Phys. Rev. B* **61** (2000) 11051.
25. J. L. Zhu, S. Zhu, Z. Zhu, Y. Kawazoe and T. Yao, *J. Phys.: Condens. Matt.* **10** (1998) L583.
26. S. T. Perez-Merchancano, H. Paredes-Gutierrez and J. Silva-Valencia, *J. Phys.: Condens. Matt.* **19** (2007) 026225.
27. P. Bhattacharya, *Semiconductor Optoelectronic Devices* (Prentice-Hall, Upper Saddle River, NJ, 1997).
28. B. R. Nag, *Physics of Quantum Well Devices* (Springer-Verlag, New York, 2002).
29. L. P. Kouwenhoven, C. M. Marcus, P. L. McEuen, S. Tarucha, R. M. Westervelt and N. S. Wingreen, in *Proc. NATO Advanced Study Institute on Mesoscopic Electron Transport*, eds. L. L. Sohn *et al.* (Kluwer Academic Publishers, Dordrecht, PAYS-BAS, 1997), pp. 105–214.